JOURNAL OF AGRICULTURAL AND FOOD CHEMISTRY

Quantification of Phenolic Compounds in Olive Oil Mill Wastewater by Artificial Neural Network/Laccase Biosensor

JOSÉ S. TORRECILLA,*,† MARIA L. MENA,§ PALOMA YÁÑEZ-SEDEÑO,§ AND JULIÁN GARCÍA†

Departments of Chemical Engineering and Analytical Chemistry, Faculty of Chemistry, Complutense University of Madrid, 28040 Madrid, Spain

In this paper is considered a new computerized approach to the determination of concentrations of phenolic compounds (caffeic acid and catechol). An integrated artificial neural network (ANN)/laccase biosensor is designed. The data collected (current signals) from amperometric detection of the laccase biosensor were transferred into an ANN trained computer for modeling and prediction of output. Such an integrated ANN/laccase biosensor system is capable of the prediction of caffeic acid and catechol concentrations of olive oil mill wastewater, based on the created models and patterns, without any previous knowledge of this phenomenon. The predicted results using the ANN were compared with the amperometric detection of phenolic compounds obtained at a laccase biosensor in olive oil wastewater of the 2004−2005 harvest season. The difference between the real and the predicted values was <0.5%.

KEYWORDS: Artificial neural network; biosensor; olive oil mill wastewater; chemical analysis; phenolic compounds

INTRODUCTION

The extraction of olive oil is achieved through discontinuous (pressing) or continuous (centrifuging) processes in traditional mills or in modern units, respectively. Centrifugation, despite its high water consumption (around 0.6 m^3 per ton of olives processed), is still the most widely employed method for the production of virgin olive oil, especially in countries that produce large amounts of olives in a short time (*1*). Usually, two byproducts are obtained with either process: a solid residue and a brownish black colored effluent from the olive plus the wash water, that is, the olive oil mill wastewater (OMW) (*2*). This liquid effluent has a high polluting organic load, due to a high content of organic substances, including sugars, tannins, polyphenols, polyalcohols, pectins, and lipids (*3*). This becomes a major environmental problem in the main olive-producing countries of the Mediterranean region. It is known that phenols are major contributors to the toxicity and the antibacterial activity of OMW, which limits its microbial degradability (*2*). Moreover, OMW may contain up to 10 g L^{-1} of phenols (*3*), the maximum amount of phenols in wastewater allowed by the European Union being <1 mg L^{-1} (Urban Water Directive 91/271/EC).

Even though there is a plethora of analytical methods for the determination of phenolic compounds, including spectrometry (*4*), high-performance liquid chromatography (*5*, *6*), gas chromatography (*7*), and gas chromatography−mass spectrometry (*8*, *9*), there is still a demand for relatively simple analytical devices, suitable for screening, and rapid assays of this type of compound in complex real samples, such as OMW. In this context, electrochemical biosensors with laccase as biological recognition element for the analysis of phenols have been developed by the immobilization of laccase on different electrode surfaces such as carbon fibers (*10*), glassy carbon (*11*, *12*), graphite (*13*−*16*), carbon paste (*17*), polyethersulfone membranes on a Universal Sensors base electrode (*18*), polyaniline-modified interdigitated Pt sensors (*19*), PVP-gel deposited on a Clark electrode (*20*), and gold surface (*21*). This kind of determination commonly uses enzymatic reactions combined with amperometric detection of the resulting product. For phenolic compounds determination, laccase is used as the enzymatic recognition part. This enzyme is well-known to reduce oxygen directly to water without the intermediate formation of hydrogen peroxide at the expense of oxidation of a variety of substrates, for example, phenols. Amperometric reduction of the generated products is then used as the quantification method, by simply applying reduction potentials. Necessary reduction potentials for this process are very near 0.0 V, which presents a great advantage as few substances interfere at this potential. The phenolic compounds tested were caffeic acid and catechol because they are two of the major phenolic compounds present in OMW (gas chromatography−mass spectrometry) and because they are two of the most sensitive substrates of laccase (*15*). Because of the similarity in the produced oxidized species, amperometric signal overlap-

* Corresponding author (telephone +34 394 42 40; fax +34 394 42 43; e-mail jstorre@quim.ucm.es).
† Department of Chemical Engineering.
§ Department of Analytical Chemistry.

10.1021/jf0703351 CCC: $37.00
Published on Web 08/08/2007

ping in the reduction voltammograms is high. This fact transforms the quantification problem into a chemometric study—a case for the application of an artificial neural network (ANN).

ANN is a mathematical algorithm that has the capability of relating input and output parameters without requiring a prior knowledge of the relationships of the process parameters. Its structure is relatively simple, with connections in parallel and sequence between neurons. This means short computing time and high potential of robustness and adaptive performance (*22*). The ANN is able to model chemical processes based on linear or nonlinear dynamics. Focusing on the chemical processes, the modeling accuracy of the ANN is comparable with that of other commercial simulators based on complex algorithms (*22*−*24*). The use of ANNs in phenolic compounds quantification has also been reported (*25*, *26*).

In this paper we present the application of ANN to the estimation of caffeic acid and catechol concentrations on a laccase biosensor based on the approximation of a relationship between input and output. The proposed integrated ANN/laccase biosensor will enable the determination of these phenolic compounds' concentrations infield and online by an ANN-trained computer. This would be very interesting for further applications to digital control, or measurement devices, which do not require any kind of mechanistic premises but only input and output variables.

EXPERIMENTAL PROCEDURES

Reagents and Solutions. Stock 0.1 mol L^{-1} solutions of caffeic acid or catechol, from Aldrich (Sigma-Aldrich Corp., St. Louis, MO), were prepared daily by dissolving the appropriate amount in methanol or water and were kept at 4 °C. More diluted standards were prepared by suitable dilution with the 0.1 mol L^{-1} citrate buffer solution (pH 5.0), which was also used as supporting electrolyte. Solutions of laccase [EC 1.10.3.2. from *Trametes versicolor*, Fluka (Riedel-de Haën, Sigma-Aldrich, Buchs, SG, Switzerland), 23.75 units mg^{-1}] were prepared in phosphate buffer solution of pH 6.5.

A 4 mM dithiobis(*N*-succinimidylpropionate) (DTSP) (Fluka) solution, prepared in dimethyl sulfoxide (DMSO) (Panreac) and stored at 4 °C, was used in the formation of the monolayer. A 25% glutaraldehyde solution (Aldrich) was also used for laccase immobilization atop the modified electrode by cross-linking. All chemicals used were of analytical reagent grade, and water was obtained from a Millipore Milli-Q (Bedford, MA) purification system.

Instrumentation and Preparation of Laccase−NTSP-Modified Gold Electrode. A Metrohm (Metrohm SA, Herisau, Swizerland) 6.1204.020 gold disc electrode (AuE) (Ø 3.0 mm) was used as the electrode substrate for further modification. A BAS MF-2063 Ag/AgCl/3 M KCl reference electrode and a Pt wire counterelectrode were also employed. A 10 mL glass electrochemical cell was used.

Preparation of Laccase−NTSP-Modified Gold Electrode. The pretreatment of the gold surface before SAMs deposition is described elsewhere (*27*). Briefly, the gold disc electrode was polished with 3.0 μm diamond powder (BAS MF-2059) for 1 min and immersed for 1 h in a hot 2 M KOH solution. Next, the electrode was rinsed with water, immersed in concentrated H_2SO_4 for 10 min, rinsed with water, immersed in concentrated HNO_3 for 10 min, and rinsed again with deionized water. Finally, the electrode was dried with argon and used immediately for the monolayer preparation.

The clean AuE was immersed in a 4 mmol L^{-1} DTSP solution in DMSO for 1 h at room temperature (*28*). Afterward, the electrode was thoroughly rinsed with water and finally with 0.1 mol L^{-1} citrate buffer (pH 5.0).

Laccase was immobilized atop the modified SAM−AuE electrode by cross-linking with glutaraldehyde by deposition of 5 μL of a 1123.5 units mL^{-1} laccase solution on the DTSP-modified AuE and subsequent immersion, once the electrode was dried out at ambient temperature, in a 25% glutaraldehyde solution for 1 h at 4 °C (*29*).

Amperometric measurement of phenolic compounds was carried out with an ECO Chemie Autolab PSTAT 10 potentiostat (Eco Chemie B.V., Utrecht, The Netherlands) using the software package GPES 4.7 (General Purpose Electrochemical System). A P-Selecta Agimatic magnetic stirrer was also used.

Amperometric sensing of phenolic compounds with the biosensor was carried out by adding different concentrations (1.0×10^{-7}−1×10^{-5} mol L^{-1}) of caffeic acid or (1.0×10^{-7}−1×10^{-5} mol L^{-1}) of catechol at 2 min intervals. Several data files were generated by injecting a measured amount of caffeic acid to a stirred solution in which the enzyme was immobilized on *N*-succinimidyl-3-thipropionate (NTSP)-modified gold electrode. Then, the electrical current generated by the concentration changes was recorded with the application of a potential of +0.00 V (*29*). The collected amperometric data were preprocessed for the ANN learning and prediction process to demonstrate the ability of ANN in model prediction of the concentration of caffeic acid or catechol of the biosensor.

Samples. OMW samples came from three different olive oil mills in Spain (Almendralejo, Badajoz; Martos, Jaén; and Villarejo de Salvanés, Madrid) and corresponded to the 2004−2005 harvest season. Olive oil was extracted using a centrifugation system in all cases.

Estimation of the Total Phenolic Compounds Content in OMW. An appropriate aliquot of homogenized sample was diluted with 10 mL of citrate buffer and transferred to the electrochemical cell. Then, while recording the current and allowing the steady state to be reached amperometric measurements were carried out in stirred solutions at 0.00 V using the laccase biosensor. For the biosensor, the content of phenolic compounds was estimated by applying the standard additions method, which implied the addition of five successive 20 μL aliquots from a 1.0×10^{-3} mol L^{-1} caffeic acid or catechol acid stock solution. For the ANN determination, the amperometric data corresponding to the addition of the sample was used to demonstrate the ability of ANN in model prediction of the concentration of phenolic compounds on the biosensor.

ANN. The type of ANN used in this work is a Perceptron model also known as backpropagation Perceptron and is probably the most commonly used today. The ANN selected is a feed-forward network with a prediction horizon and supervised learning. It is characterized by layered architectures, and feed-forward connections between neurons, or back connections, are possible. Weights are assigned to these connections between the neurons of one layer and the next. To predict with the least possible error, these values were optimized. This type of network has been selected because it is a good pattern classifier, signal filter, and data compressor (*30*). Specifically, the backpropagation Perceptron multilayer is used to model systems based on nonlinear dynamics (*22*, *24*, *25*, *31*). On the other hand, another important advantage is that knowledge of the system to be modeled is not necessary; therefore, the ANN has enormous applicability. The ANN used was designed by Matlab version 7.01.24704 (R14). The statistical analyses were carried out by Statgraphics Plus (version 5.1). The ANN consists of two layers with connections to the outside world (an input layer by which data are presented to the network and an output layer that holds the network response to given inputs) and one hidden layer (optimized afterward). The variables input into the ANN must be characteristic of the system. The output layer consists of two neurons for the output variables; that is, the ANN predicts the caffeic acid and catechol concentrations. This topology with a single hidden layer has been considered sufficient to solve similar or more complex problems (*22*, *24*, *25*). Moreover, more hidden layers may cause overfitting (*32*).

The transfer function (TF) used in ANN, the number of hidden neurons, and other parameters of the ANN are optimized below. The learning and verification samples and processes are described below and, then, an optimization process is exposed.

Learning and Verification Sample. The learning sample was used to optimize the weights, that is, select the adequate matrix of weights to predict, with the least possible error, the real value by the input values. On the other hand, the verification sample was used in the verification process. At this stage, the ANN uses the input values to estimate the output values, and no optimization process of weights was carried out. These samples were composed of data that characterized the process. They have as many rows as variables necessary to model

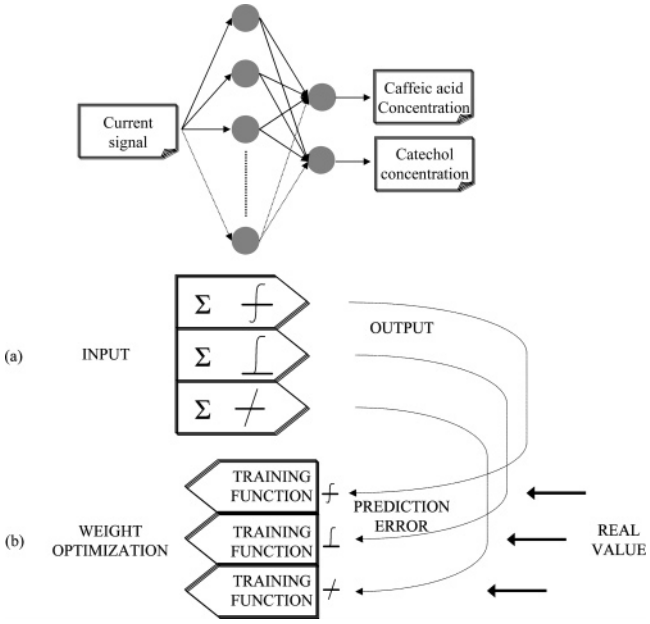

Figure 1. Schematic diagram of calculation in a backpropagation Perceptron: (**a**) prediction stage and first part of optimization process of the weights; (**b**) second part of weight optimization.

the process and the same number of columns as the number of vectors to describe the system to measure. The independent variables that characterize the process to be modeled are laccase units, pH value, and applied potential and current signal. Given that the ANN was applied to three specific OMWs (Almendralejo, Badajoz; Martos, Jaén; and Villarejo de Salvanés, Madrid) for which the laccase units, pH value, and potential value were fixed to 6, 5, and 0 V, respectively, the learning sample is composed of three rows, that is, current signal (μA) and caffeic acid and catechol concentration values (μM), and its number of columns was 300. Every sample had the same format and was normalized in the range from 0 to 1 or from −1 to 1 depending on the TF used (sigmoid or hyperbolical tangent and lineal pendant functions, respectively). The difference between samples is the percentage of data used in each one; that is, the learning and verification sample have 80 and 20% of the total data, respectively. Taking into account that every datum (current signal and caffeic acid and catechol concentration values) of the verification sample should be interpolated within learning range, the data were randomly distributed in both samples.

Learning and Verification Processes of ANN. The development of ANN involves two basic steps, learning and verification processes.

(a) Learning Process. The learning sample set was presented to the network, and a backpropagation algorithm automatically adjusted the weights; therefore, the output response to input vector was as close as possible to the desired response (*33*) (**Figure 1a**). Each time an estimation was made, the result was compared to the corresponding desired value. Then, the estimation error (the difference between the estimated and real values, also called the prediction error) was backdistributed across the network in a manner that allowed the interconnection weights to be modified according to the scheme specified by the learning rule (**Figure 1b**). To optimize the ANN, several training functions were tested. They are summarized in **Table 1**. These are classified as a function of the algorithm type used to update the matrix of weights of the ANN. When the weights were modified, the next data set was fed to the network, and a new estimation was made. The estimation error was calculated again and backdistributed across the network for the next modification. Simultaneously, using the verification sample, a verification test was carried out to determine the level of generalization produced by the learning set and to monitor ANN overfitting (*34*). When every datum of the learning sample was used, an epoch was finished and other one began. To avoid the overfitting of the neural network model, the learning process was repeated while the verification error decreased (*35*).

Table 1. Summary of All Tested Training Functions (*36*)

training function	description
	Gradient Descent with Variable Learning Rate
TRAINGD	gradient descendent backpropagation (BP)
TRAINGDM	gradient descendent with momentum BP
TRAINGDX	gradient descendent with momentum and adaptive linear BP
TRAINGDA	gradient descendent with adaptive learning learning rate BP
	Conjugated Gradient Descent
TRAINCGF	Fletcher Powell conjugate gradient BP
TRAINCGP	Polak–Ribiere conjugate gradient BP
TRAINCGB	Powell–Beale conjugate gradient BP
TRAINSCG	scaled conjugate gradient BP
	Quasi-Newton Algorithm
TRAINBFG	BFGS quasi-Newton BP
TRAINOSS	one-step secant BP
	Resilient Backpropagation
TRAINR	random order incremental update
TRAINRP	resilient PB (Rprop)
	Levenberg–Marquardt
TRAINLM	Levenberg–Marquard BP
	Automated Regularization
TRAINBR	Bayesian regularization

Among other parameters of the ANN, the number of neurons in the hidden layer is related to the converging performance of the output error function during the learning process of the network; the learning coefficient (Lc) controls the degree at which connection weights are modified during the learning phase.

(b) Verification Process. The objective of this step was to evaluate the competence of the trained network. For each training function, the matrix of weight optimized above was used. The verification sample was input into the ANN, and predicted values were calculated (**Figure 1a**). In the verification process, these were compared with the real ones to optimize the parameters of the ANN by statistical tools and to test the ANN. In this process, no corrections of these weights were made and the ANN was used only to predict.

Optimization Process of the ANN. To optimize the ANN, two stages were carried out. First, the adequate training function was selected, and then the main parameters of the ANN (using the selected training function) were optimized. Finally, these two stages were repeated to select the adequate TF (sigmoid, hyperbolical tangent, or linear transfer function).

(a) Selection of the Training Function. Using the adequate learning and verification samples, the training function was selected from among 14 different functions (**Table 1**). To investigate the effect of each training function, all other ANN parameters were set; that is, the topology was five hidden neurons, and the others were set as shown in the literature (*36*). With these conditions and for each training function, a learning process (using 100 epochs) and, then, a verification process were developed. This process was repeated for every training function and, then, all predicted values for each training function were compared one by one with the real values. These comparisons were carried out by prediction error, statistical tests, and correlation coefficients (real vs predicted values) (R^2 values). The statistical analysis was carried out to determine if there were significant differences between real data and those predicted by the ANN (at a 95% confidence level). The null hypothesis assumes that statistical parameters of both series are equal. Otherwise, an alternative hypothesis is defined. The p value was used to check each hypothesis. Its threshold value was 0.05. If the p value is greater than this, the null hypothesis is fulfilled. Different parametric and nonparametric methods were applied on the basis of measure of either central tendency (Kolmogorow−Smirnov test, Mann−Whitney−Wilcoxon test, and Kruscal−Wallis test), variance (Kruscal−Wallis test, Cochran C test, Barllet's test, and Levene test), or inferential parametric test for significance (F test and t test). In every case, the p values of

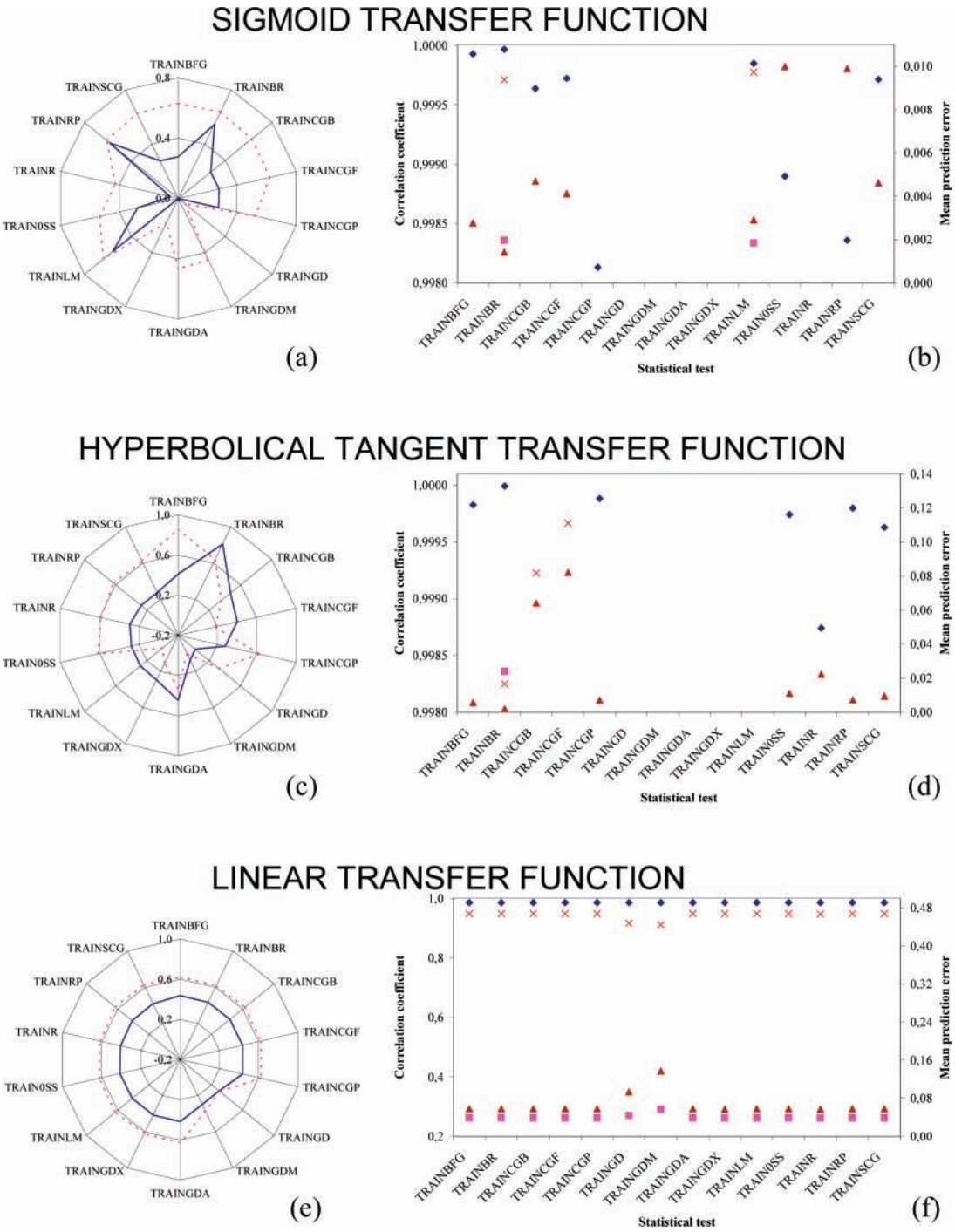

Figure 2. Training function selection process: (**a**, **c**, **e**) mean *p* value (- - -, caffeic acid; —, catechol); (**b**, **d**, **f**) R^2 (◆, caffeic acid; ■, catechol) and MPE (▲, caffeic acid; ×, catechol).

statistical tests developed were >0.05. Therefore, the mean *p* value can be calculated as a representative value.

Given that the ANN should predict with the highest possible accuracy, the training function selection was carried out to obtain the least prediction error and the highest values of *p* value and R^2 (real vs predicted values).

Optimization of ANN Parameters. Using the ANN with the training function selected above, the parameters of the ANN were optimized by experimental design. The experimental design was a central composite design 2^4 + star. Taking the selected training function into account, the variables analyzed were the hidden neurons number (topology), Lc, Lcd, and Lci, and the responses were taken in the learning and verification processes: in the learning process, the epoch number necessary to optimize the matrix of weights was taken, and in the verification process, the R^2 (real vs predicted values) one for each output neurons (caffeic acid and catechol compounds) and mean prediction error (MPE) were calculated.

The hidden neurons were tested between 5 and 15 neurons, because when the number of hidden neurons is smaller than 5 the ANN is not able to adapt to the process to be modeled, and when it is higher than 15 the number of parameters to optimize in each epoch is over 45. The Lci was tested between 2 and 100; Lc and Lcd were tested between 0.001 and 1 (*37*). A learning process was carried out in each run of the experimental design. Then, the verification process was carried out using the matrix of weights optimized in its learning process. Finally, the responses of experimental design were taken. The design was analyzed by taking into account that requirement that the ANN should predict with the least prediction error and both R^2 values must be as close to unity as possible in the lowest iteration number.

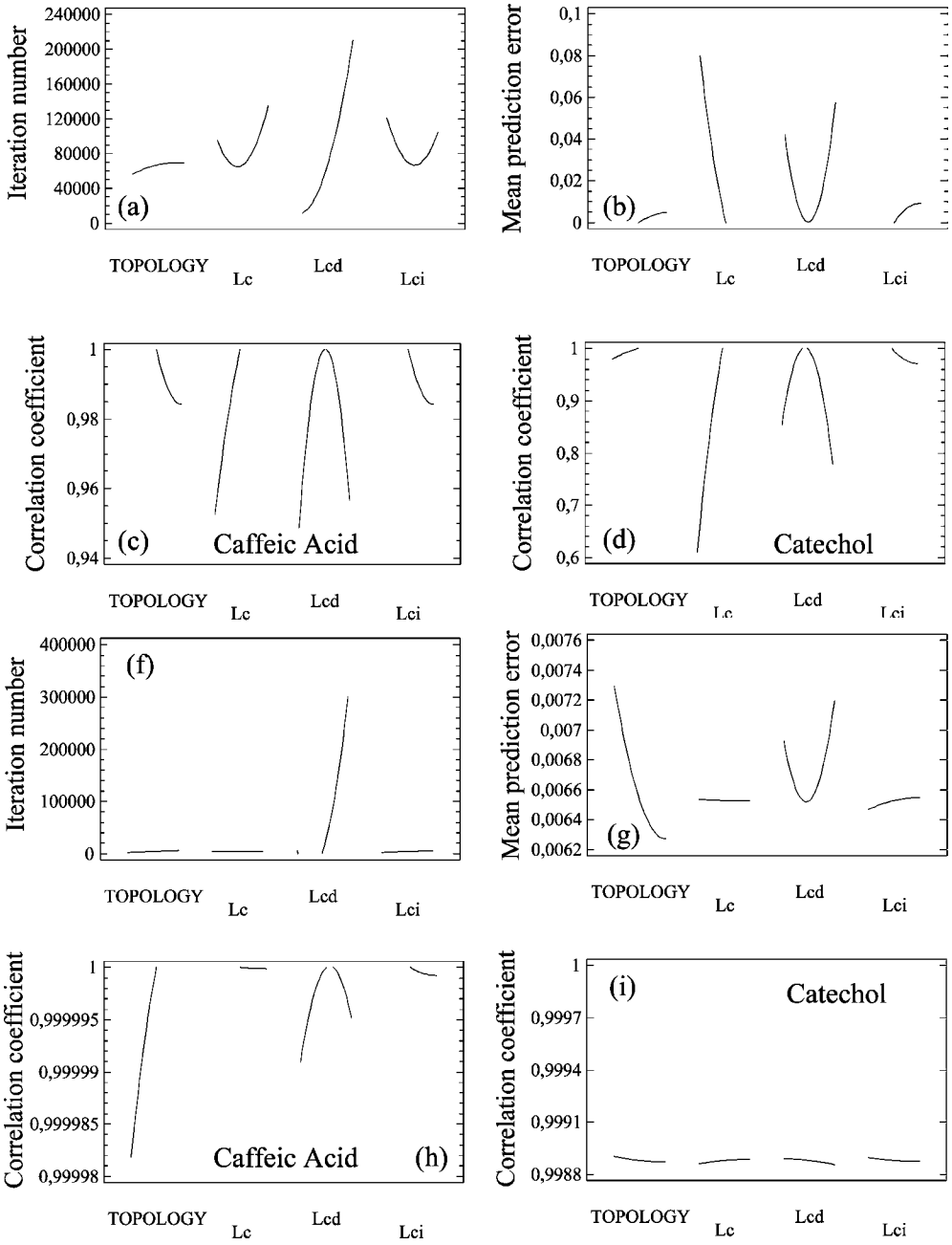

Figure 3. Analysis of influences of factor on the responses: (**a**–**d**) predictions carried out by ANNS; (**f**–**i**) estimations carried out by ANNH.

Testing of the Optimized ANN. The verification sample was input into the optimized ANN, and then its prediction and real values were checked. The evaluation of the ANN consisted of calculating of prediction error, both R^2 values (real vs predicted values) and p values of statistical tests. As has been shown under Selection of Training Function, the statistical analysis was carried out by calculating and comparing the p value with the threshold (0.05) in parametric and nonparametric statistical tests (Kolmogorow−Smirnov, Mann−Whitney−Wilcoxon, Kruscal−Wallis, Kruscal−Wallis, Cochran C, Barllet's, Levene, F test, and t test).

RESULTS AND DISCUSSION

Training and Transfer Function Selection. The learning and verification processes were carried out using a sigmoid, hyperbolical tangent and linear TFs. In the verification process, the selection of adequate TF was carried out by comparing the prediction error of two ANNs by statistical tools. The ANN using the sigmoid function (ANNS), hyperbolical function (ANNH), and linear transfer (ANNL) as TF are described below.

Sigmoid Transfer Function. To optimize the ANNS, the current signal was input into the ANNS, and the output was composed of caffeic acid and catechol concentrations. The calculation process followed to optimize the ANNS is described under Optimization Process of the ANN.

From a p value point of view, focusing attention on the caffeic acid concentration prediction, the two best training functions were TRAINLM and TRAINBR. With the catechol concentration estimation as the focus, the best training functions were TRAINLM, TRAINBR and TRAINRP (**Figure 2a**). From R^2 and MPE points of view, the best results were taken using an ANNS with TRAINBR (**Figure 2b**). Given that the ANN should predict both variables as well as possible, the TRAINBR was selected as training function.

The influences of every factor over the response of the experimental design were analyzed (**Figure 3**). The topology is the factor with the most influence over $R^2_{\text{caffeic acid}}$ (real vs predicted values). The Lc has a notable influence over MPE

Table 2. Parameters of the ANN, Final Prediction Error Depending on the Transfer Function Used (with a 95% Confidence Level)

	ANNS	ANNH	ANNL
Optimized Parameters of the ANN			
training function	TRAINBR		
hidden neurons number	10	20	10
learning coefficient	0.5005	0.5005	0.5005
learning coefficient decrease	0.5005	0.5005	0.5005
learning coefficient increase	149	51	149
Final Prediction Error			
MPE	5.1×10^{-4}	6.5×10^{-3}	2.6×10^{-1}
sum of prediction error	3.3×10^{-2}	4.5×10^{-1}	1.7×10^{1}
mean R^2	>0.999	>0.999	0.765
Calculated Parameters of the ANN			
hidden neurons number	7		
learning coefficient	1		
learning coefficient decrease	0.879		
learning coefficient increase	117		
Final Prediction Error			
MPE	3.1×10^{-3}		
sum of prediction error	2×10^{-2}		
mean R^2	>0.999		

and both R^2 values. The Lcd is the factor with most influence over all responses of experimental design. Finally, Lci has influence over the $R^2_{\text{caffeic acid}}$. Given that the factors with more influence are Lc and Lcd, if a global method of improving the ANNS prediction were necessary, it would consist of carrying out a fine-tuning of Lc and Lcd. This tuning could be made easy if the their response surface was known. Therefore, the influence of Lc and Lcd on every response of experimental design is shown in **Figure 4**. As can be seen, from MPE and both R^2 values points of view, the best results are reached when Lcd and Lc are ≥ 0.5. Nevertheless, the optimized parameter values are calculated in a different way.

The parameters of the ANN with TRAINBR training function were optimized by an experimental design. Taking into account the considerations described above, the optimized parameters are 10 hidden neurons, Lc and Lcd = 0.5005 and Lci = 149 were the optimal values of the ANNS. In the verification process, the mean R^2 of both estimations (caffeic acid and catechol concentrations) was >0.999 and the MPE was 5.1×10^{-4} (**Table 2**). Therefore, the ANNS is able to predict the caffeic acid and catechol concentrations.

Another method to calculate the optimal parameters values was used. The experimental design responses were fitted to four regression equations (eq 1). Then, the optimal parameters of the ANN were calculated by solving this system of equations

$$\begin{pmatrix} -1507.28 & 54909.30 & 198765.00 & -44.95 \\ 1.5 \times 10^{-4} & -9.4 \times 10^{-2} & 1.5 \times 10^{-2} & 1.7 \times 10^{-4} \\ 7.0 \times 10^{-3} & 4.6 \times 10^{-1} & -7.5 \times 10^{-2} & -4.1 \times 10^{-4} \\ -4.6 \times 10^{-3} & 5.5 \times 10^{-2} & 7.8 \times 10^{-3} & -4.7 \times 10^{-4} \end{pmatrix} \begin{pmatrix} \text{topology} \\ \text{Lc} \\ \text{Lcd} \\ \text{Lci} \end{pmatrix} + \begin{pmatrix} 76342.8 \\ 8.2 \times 10^{-2} \\ 7.0 \times 10^{-3} \\ 1.0162 \end{pmatrix} = \begin{pmatrix} \text{iteration} \\ \text{MPE} \\ R^2_{\text{catechol}} \\ R^2_{\text{caffeic acid}} \end{pmatrix} \quad (1)$$

where every variable is specified in its original unit. The required response values were interpolated inside the range of experimental design run results and agreed with the assumed considerations (**Table 3**) (for example, the selected MPE was 1.5×10^{-4} because the least prediction error value is required).

Table 3. Response Ranges of Experimental Design Runs and Their Required Values

	max value	min value	mean value	required value
Sigmoid Transfer Function				
iteration	300000	149000	187626	149000
MPE	2.2×10^{-1}	5.1×10^{-4}	4.8×10^{-2}	5.1×10^{-4}
$R^2_{\text{caffeic acid}}$	>0.999	0.716	0.976	1
R^2_{catechol}	>0.999	0.172	0.778	1
Tangent Hyperbolical Transfer function				
iteration	300000	4125	117406	4125
MPE	6.5×10^{-3}	8.3×10^{-3}	7.11×10^{-3}	8.3×10^{-3}
$R^2_{\text{caffeic acid}}$	>0.999	>0.999	>0.999	1
R^2_{catechol}	0.999	0.998	0.998	1

The solution of the system of equations was learning sample of seven hidden neurons, Lc, Lcd, and Lci equal to 1, 0.879, and 117, respectively. Finally, these values were tested in the ANNS, and the results are shown in **Table 2**. Given that in the prediction process there are two-factor interactions, the MPE value (3.1×10^{-3}) is higher than the required value (5.1×10^{-4}).

Hyperbolical Tangent Transfer Function. The calculation process was explained under Optimization Process of ANN. Following this method, the mean of *p* values were calculated. The mean *p* values, the R^2 values, and MPE versus training function are shown in **Figure 2**. The *p* values of real and predicted values calculated by TRAINBFG and TRAINBR training functions were the closest to unity (**Figure 2a**). From MPE and R^2 points of view, the estimations calculated using TRAINBR are the best. Therefore, it was selected.

The influences of every independent variable on the responses of the experimental design were studied (**Figure 3**). The topology has influence on MPE and caffeic acid coefficient correlation (real vs predicted values). The Lc has a slight influence on both R^2 values. The Lcd is the factor with most influence over every independent variable. Finally, Lci has influence over the MPE and R^2_{catechol}. Given that the factors having the most influence are topology and Lcd, a fine-tuning of these factors could improve the ANNH estimations, if it would be necessary. The fine adjustment of these could be made easy if the response surface was known. Therefore, the influence of these on every response of experimental design is shown in **Figure 4**. As can be seen, the topology and Lcd could be calculated by local extremes of the response surfaces. However, the optimized values of the independent variables were calculated in a different way.

The experimental design was carried out in the same way and by taking into account the same considerations as in the subsection above. The optimal values and the main results are shown in **Table 2**.

To calculate the optimal parameters of the ANNH, the system of equations (eq 2) formed by the fit of the responses of experimental design was solved

$$\begin{pmatrix} -1967.95 & -23024.30 & 295230.00 & -211.172 \\ 9.5 \times 10^{-5} & -1.4 \times 10^{-4} & 2.7 \times 10^{-4} & -6.7 \times 10^{-7} \\ 2.5 \times 10^{-6} & 2.0 \times 10^{-5} & -3.4 \times 10^{-5} & -1.8 \times 10^{-7} \\ -2.1 \times 10^{-6} & 1.7 \times 10^{-6} & 4.2 \times 10^{-6} & -3.4 \times 10^{-9} \end{pmatrix} \begin{pmatrix} \text{topology} \\ \text{Lc} \\ \text{Lcd} \\ \text{Lci} \end{pmatrix} + \begin{pmatrix} 14633.8 \\ 8.1 \times 10^{-3} \\ 9.9 \times 10^{-1} \\ 9.9 \times 10^{-1} \end{pmatrix} = \begin{pmatrix} \text{iteration} \\ \text{MPE} \\ R^2_{\text{catechol}} \\ R^2_{\text{caffeic acid}} \end{pmatrix} \quad (2)$$

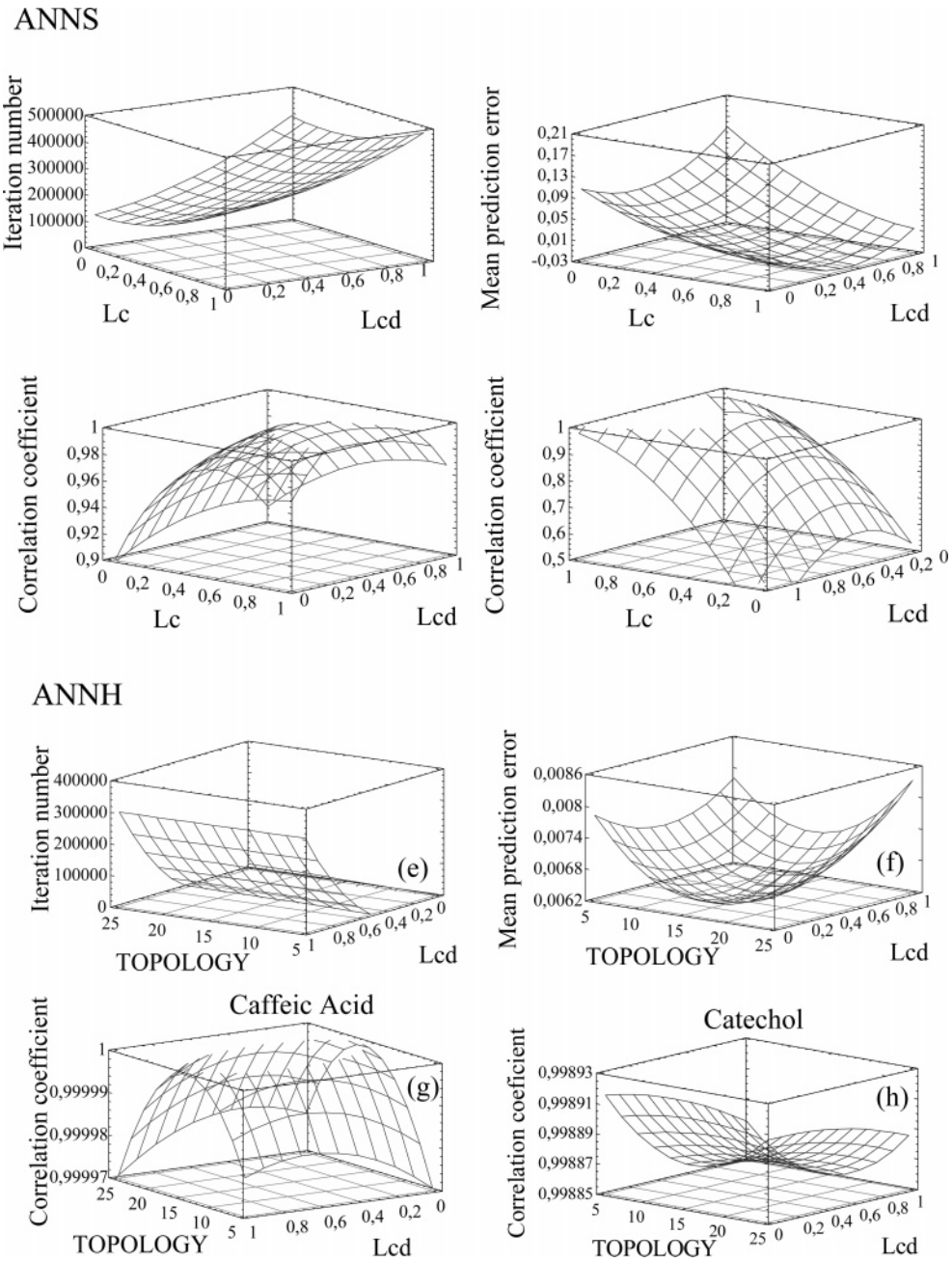

Figure 4. Response surfaces of experimental design variables: (**a**–**d**) predictions carried out by ANNS; (**f**–**i**) estimations carried out by ANNH.

where every variable is specified in its original unit. The required response values were taken using the same method described under Sigmoid Transfer Function. Given that the two-factor interaction effects are not negligible, the solution of equations system is outside the studied range. Therefore, the optimal parameter values were not calculated by this method.

Linear Transfer Function. The calculation process followed to optimize the ANNL is the same as the two other ANNs described above. The best estimation of caffeic acid and catechol concentrations was reached using any tested training function except TRAINGD and TRAINGDM. Given that TRAINBR was selected in both studied ANNs, this training function was also selected in ANNL (**Figure 2**). Using the same experimental design method and taking into account the same considerations described above, the optimized parameters were calculated and the main results are shown in **Table 2**.

Given that the relationship between real current signal and real concentration data is a nonlinear dependence, the ANNL, based on lineal relation, is not adequate. Because of this, the MPE values are the highest and the R^2 is the lowest. Therefore, the influence analysis was not carried out.

Transfer Function Selection. Given that the optimized ANN was used to predict caffeic acid and catechol concentrations, the lowest MPE and highest R^2 were the criteria to select the adequate ANN (ANNH or ANNS). As can be seen in **Table 2**, the mean R^2 values were similar in both cases, but the mean and the sum prediction error values (sum of prediction error values in the verification process for every data set) calculated by ANNS were less than the other. Therefore, the ANN selected to predict the caffeic acid and cathecol concentrations was the ANNS.

Application of ANNS to a Real Case. Finally, to validate the prediction capability of the optimized ANNS, other verification data were made (*38*), formed by current signal and caffeic

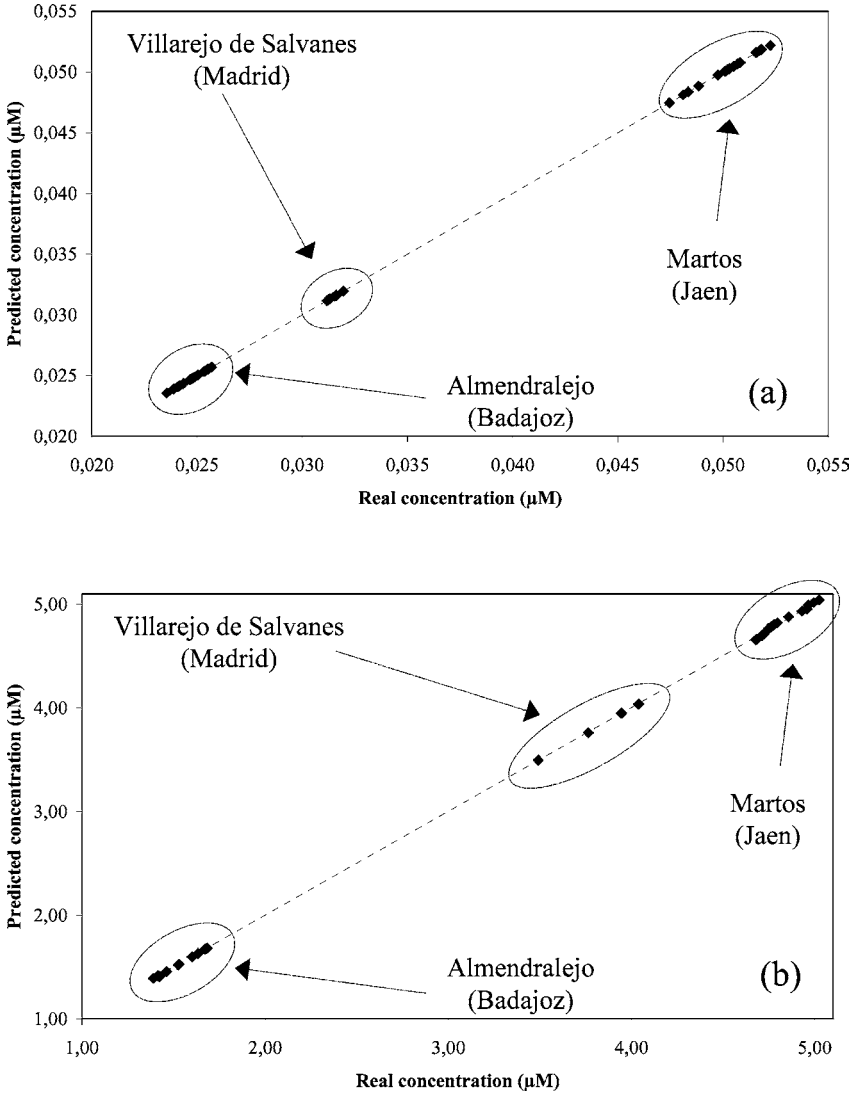

Figure 5. Predicted and real concentration values taken from three different olive oil mills in Spain (- - -, lineal fit): (**a**) caffeic acid ($R^2 > 0.999$); (**b**) catechol ($R^2 > 0.999$).

acid and catechol concentration values. These were taken from three different olive oil mills in Spain (Almendralejo, Badajoz; Martos, Jaén; and Villarejo de Salvanés, Madrid) by field measurement. As can be seen in **Figure 5**, both R^2 values (real vs predicted values) are >0.999 and the MPE is <0.5%.

Both series of predicted and real values (caffeic acid and catechol compounds) were compared by statistical analysis, and the mean *p* value was >0.87. Given that it was >0.05, there is not a statistically significant difference between the two distributions (real and predicted values) with a 95% confidence level.

To sum up, the optimized ANNS is able to calculate the caffeic acid and catechol concentrations when the ANNS is used within the range studied.

Conclusion. An artificial neural network has been optimized and validated. The data samples used to carry out the learning and verification processes were taken from three mills in Spain (Almendralejo, Badajoz; Martos, Jaén; and Villarejo de Salvanes, Madrid) by field measurement. The training and transfer functions of the ANN were optimized. The ANN used was implemented with a sigmoid transfer function and a TRAINBR training function (Lc and Lcd = 0.5005 and Lci = 149). The ANNS topology had an input node (current signal), 10 hidden and 2 output neurons (caffeic acid and catechol concentrations). The mean difference between the real and the predicted values of caffeic acid and catechol concentrations was <0.5%. Given that the mean *p* value is >0.87, there is no statistical difference between these real and predicted concentrations.

The ANN/laccase biosensor can be adapted to quantify caffeic acid and catechol concentrations and to deconvolute the contribution of each one. Given that this prototype is able to model the process to be measured with accuracy, it has the advantage of being more selective and more accurate than conventional methods.

To sum up, the ANN is an adequate tool to estimate the concentration of a pollutant with a high environmental impact in olive oil mill wastewater, without any previous phenomenological knowledge.

LITERATURE CITED

(1) Benitez, J.; Beltran-Heredia, J.; Torregrosa, J.; Acero, J. L.; Cercas. V. Aerobic degradation of olive mill wastewaters. *Appl. Microbiol. Biotechnol.* **1997**, *47* (2), 185−188.

(2) Borja, R.; Alba, J.; Banks, C. J. Impact of the main phenolic compounds of olive mill wastewater (OMW) on the kinetics of acetoclastic methanogenesis. *Process Biochem.* **1997**, *32* (2), 121−133.

(3) D'Annibale, A.; Crestini, C.; Vinciguerra, V.; Sermanni, G. G. The biodegradation of recalcitrant effluents from an olive mill by a white-rot fungus. *J. Biotechnol.* **1998**, *61* (3), 209−218.

(4) Bosch, F.; Font, G.; Manes, J. Ultraviolet spectrophotometric determination of phenols in natural and waste waters with iodine monobromide. *Analyst* **1987** *112* (9), 1335−1337.

(5) Ong, C. P.; Lee, H. K.; Li, S. F. Y. Optimization of mobile phase-composition for high-performance liquid-chromatographic analysis of 11 priority substituted phenols. *J. Chromatogr.* **1989**, *464* (2), 405−410.

(6) Zhao, L. M.; Lee, H. K. Determination of phenols in water using liquid phase microextraction with back extraction combined with high-performance liquid chromatography. *J. Chromatogr., A* **2001**, *931* (1−2), 95−105.

(7) Bartak, P.; Frnkova, P.; Cap, L. Determination of phenols using simultaneous steam distillation-extraction. *J. Chromatogr., A* **2000**, *867* (1−2), 281−287.

(8) Angerosa, F.; Dalessandro, N.; Konstantinou, P.; Digiacinto, L. GC-ris evaluation of phenolic-compounds in virgin olive oil. *J. Agric. Food Chem.* **1995**, *43*, 1802−1807.

(9) Tasioula-Margari, M.; Okogeri, O. Isolation and characterization of virgin olive oil phenolic compounds by HPLC/UV and GC-MS. *J. Food Sci.* **2001**, *66* (4), 530−534.

(10) Freire, R. S.; Duran, N.; Kubota, L. T. Development of a laccase-based flow injection electrochemical biosensor for the determination of phenolic compounds and its application for monitoring remediation of Kraft E1 paper mill effluent. *Anal. Chim. Acta* **2002**, *463* (2), 229−238.

(11) Freire, R. S.; Thongngamdee, S.; Duran, N.; Wang J.; Kubota, L. T. Mixed enzyme (laccase/tyrosinase)-based remote electrochemical biosensor for monitoring phenolic compounds. *Analyst* **2002**, *127* (2), 258−261.

(12) Leech, D.; Daigle, F. Optimisation of a reagentless laccase electrode for the detection of the inhibitor azide. *Analyst* **1998**, *123* (10), 1971−1974.

(13) Kulys, J.; Vidziunaite, R. Amperometric biosensors based on recombinant laccases for phenols determination. *Biosens. Bioelectron.* **2003**, *18* (2−3), 319−325.

(14) Yaropolov, A. I.; Kharybin, A. N.; Emneus, J.; Markovarga, G.; Gorton, L. Flow-injection analysis of phenols at a graphite electrode modified with co-immobilized laccase and tyrosinase. *Anal. Chim. Acta* **1995**, *308* (1−3), 137−144.

(15) Haghighi, B.; Gorton, L.; Ruzgas, T.; Jönsson, L. J. Characterization of graphite electrodes modified with laccase from *Trametes versicolor* and their use for bioelectrochemical monitoring of phenolic compounds in flow injection analysis. *Anal. Chim. Acta* **2003**, *487* (1), 3−14.

(16) Jarosz-Wilkolazka, A.; Ruzgas, T.; Gorton, L. Use of laccase-modified electrode for amperometric detection of plant flavonoids. *Enzyme Microb. Technol.* **2004**, *35* (2−3), 238−241.

(17) Leite, O. D.; Lupetti, K. O.; Fatibello, O.; Vieira, I. C.; Barbosa, A. D. Synergic effect studies of the bi-enzymatic system laccase-peroxidase in a voltammetric biosensor for catecholamines. *Talanta* **2003**, *59* (5), 889−896.

(18) Gomes, S. A. S. S.; Rebelo, M. J. F. A new laccase biosensor for polyphenols determination. *Sensors* **2003**, *3* (6), 166−175.

(19) Timur, S.; Pazarlioglu, N.; Pilloton, R.; Telefoncu, A. Thick film sensors based on laccases from different sources immobilized in polyaniline matrix. *Sens. Actuators, B: Chem.* **2004**, *97* (1), 132−136.

(20) Roy, J. J.; Abraham, T. E.; Abhijith, K. S.; Sijithkumar, P. V.; Thakur, M. S. Biosensor for the determination of phenols based on cross-linked enzyme crystals (CLEC) of laccase. *Biosens. Bioelectron.* **2005**, *21*, 206−211.

(21) Vianello, F.; Cambria, A.; Ragusa, S.; Cambria, M. T.; Zennaro, L.; Rigo, A. A high sensitivity amperometric biosensor using a monomolecular layer of laccase as biorecognition element. *Biosens. Bioelectron.* **2004**, *20*, 315−321.

(22) Palancar, M. C.; Aragón, J. M.; Torrecilla, J. S. pH-Control system based on artificial neural networks. *Ind. Eng. Chem. Res.* **1998**, *37*, 2729−2740.

(23) Torrecilla, J. S.; Otero, L.; Sanz, P. D. Artificial neural networks: a promising tool to design and optimize high-pressure food processes. *J. Food Eng.* **2005**, *69*, 299−306.

(24) Torrecilla, J. S.; Aragón, J. M.; Palancar, M. C. Modeling the drying of a high-moisture solid with an artificial neural network. *Ind. Eng. Chem. Res.* **2005**, *44*, 8057−8066.

(25) Trojanowicz, M.; Jagielska, A.; Rotkiewicz, P.; Kierzek, A. Flow-injection determination of phenols with tyrosinase amperometric biosensor and data processing by neural network. *Chem. Anal.* **1999**, *44*, 865−878.

(26) Gutés, A.; Céspedes, F.; Alegret, S.; Valle, M. Determination of phenolic compounds by a polyphenol oxidase amperometric biosensor and artificial neural network analysis. *Biosens. Bioelectron.* **2005**, *20*, 1668−1673.

(27) Campuzano, S.; Gálvez, R.; Pedrero, M.; Manuel de Villena, F. J.; Pingarrón, J. M. Preparation, characterization and application of alkanethiol self-assembled monolayers modified with tetrathiafulvalene and glucose oxidase at a gold disk electrode. *J. Electroanal. Chem.* **2002**, *526*, 92−100.

(28) Darder, M.; Takada, K.; Pariente, F.; Lorenzo, E.; Abruña, H. D. Dithiobissuccinimidyl propionate as an anchor for assembling peroxidases at electrodes surfaces and its application in a H_2O_2 biosensor. *Anal. Chem.* **1999**, *71*, 5530−5537.

(29) Mena, M. L.; Carralero, V.; González-Cortés, A.; Yáñez-Sedeño, P.; Pingarrón, J. Laccase biosensor based on *N*-succinimidyl-3-thiopropionate-functionalized gold electrodes. *Electroanalysis* **2005**, *17*, 2147−2155.

(30) Maren, A. J.; Harston, T.; Pap, R. P. *Handbook of Neural Computing Applications*; Academic Press: San Diego, CA, 1990; pp 323−324.

(31) Torrecilla, J. S.; Otero, L.; Sanz, P. D. A neural network approach for thermal/pressure food processing. *J. Food Eng.* **2004**, *62*, 89−95.

(32) Ruan, R.; Almaer, S.; Zhang, J. Prediction of dough rheological properties using neural networks. *Cereal Chem.* **1995**, *72* (3), 308−311.

(33) Ni, H.; Gunasekaran, S. Food quality prediction with neural networks. *Food Technol.* **1998**, *52* (10), 60−65.

(34) Ghaffari, A.; Abdollahi, H.; Khoshayand, M. R.; Soltani Bozchalooi, I.; Dadgar, A.; Rafiee-Tehrani, M. Performance comparison of neural network training algorithms in modeling of bimodal drug delivery. *Int. J Pharm.* **2006**, *327* (1−2), 126−138.

(35) Izadifar, M.; Abdolahi, F. Comparison between neural network and mathematical modeling of supercritical CO_2 extraction of black pepper essential oil. *J. Supercrit. Fluids* **2006**, *38* (1), 37−43.

(36) Demuth, H.; Beale, M.; Hagan, M. *MATLAB User's Guide, v 4.0: Neural Network Toolbox*; MathWorks Inc.: Natick, MA, 2005.

(37) Vacic, V. Summary of the training functions in Matlab's NN toolbox; 2005; http://www.cs.ucr.edu/~vladimir/cs171/nn_summary.pdf.

(38) Singleton, V. L.; Rossi, J. A. Colorimetry of total phenolics with phosphomolybdic−phosphotungstic acid reagents. *Am. J. Enol. Vitic.* **1965**, *16*, 144−158.

Received for review February 6, 2007. Revised manuscript received June 7, 2007. Accepted June 26, 2007. We are grateful to the Ministerio de Educación y Ciencia for financial support (Project CTQ2006-04644). J.S.T. was supported by a Ramón y Cajal research contract from the Ministerio de Educación y Ciencia in Spain.

JF0703351